

Measurement of the temperature and the pumping uniformity inside a Nd:YAG rod by an interferometric method

Kwang Suk Kim, Hong Jin Kong, and Cheol Jung Kim

Citation: *Appl. Phys. Lett.* **58**, 1810 (1991); doi: 10.1063/1.105096

View online: <http://dx.doi.org/10.1063/1.105096>

View Table of Contents: <http://apl.aip.org/resource/1/APPLAB/v58/i17>

Published by the [American Institute of Physics](#).

Additional information on *Appl. Phys. Lett.*

Journal Homepage: <http://apl.aip.org/>

Journal Information: http://apl.aip.org/about/about_the_journal

Top downloads: http://apl.aip.org/features/most_downloaded

Information for Authors: <http://apl.aip.org/authors>

ADVERTISEMENT



Goodfellow
metals • ceramics • polymers • composites
70,000 products
450 different materials
small quantities fast

www.goodfellowusa.com

Measurement of the temperature and the pumping uniformity inside a Nd:YAG rod by an interferometric method

Kwang Suk Kim and Hong Jin Kong

Department of Physics, Korea Advanced Institute of Science and Technology, 373-1 Kusung-dong
Yoosung-ku, Daejeon, Korea

Cheol Jung Kim

Electro-Optics Department, Korea Atomic Energy Research Institute, KAERI P. O. Box 7,
Dae-Duk Science Town, Daejeon, Korea

(Received 18 September 1990; accepted for publication 4 March 1991)

The thermal behavior of a Nd:YAG laser rod under flashlamp pumping has been investigated experimentally using a very simple interferometric technique. The degree of pumping uniformity and the heat generation rate inside the rod was evaluated for single pulse pumping. The temperature increase at the center of the rod under a high repetition rate pulsed operation was also measured, and this result is used to deduce the surface heat transfer coefficient.

The problem of managing the thermal energy deposited inside a solid-state laser rod under high power and high repetition rate optical pumping has long been of critical importance in the design of an industrial solid-state laser. Thermal effects which stem from the temperature gradient inside the laser rod as a result of the cooling process and nonuniform pumping are mainly responsible for the optical distortions of the laser beam.

The thermal behavior of a rod during pumping has been widely investigated in determining the variations of the optical length.^{1,2} Cabezas *et al.*³ measured the optical length variation during single pulse pump period using the interferometric method in their early work. Mangir and Rockwell⁴ have measured the heat deposited in the uncooled rod. Mann and Weber⁵ obtained the surface heat transfer coefficient (SHTC) and the heat generation efficiency of inside the rod for a single pulse operation. The time-dependent temperature distribution of an infinitely long laser rod with a uniformly generated heat source has also been studied theoretically by Koehnner,⁶ and that for a rod of finite length has been derived by Farrukh *et al.*⁷ Recently, a comparative study of different pumping reflectors has been made by Docchio *et al.*⁸ and by Milev *et al.*⁹ Their results seem to be inconclusive in finding a relationship between the pumping geometry and the intensity profile of the laser beam.

In our experiments, we measured the spatial temperature distribution and the heat generation rate (HGR) inside the rod after single pulse pumping. Moreover, the temperature rise at the center of the water cooled rod for a high repetition rate pulsed operation was also measured using a simple interferometric technique. With these results, we easily deduced the SHTC of the rod, which allows the prediction of the temperature of a multikilowatt-pumped Nd:YAG rod. Consequently, we were able to evaluate the practical parameters such as the transverse pumping uniformity and temperature rise of the rod under high power and high repetition rate pulsed operation.

Figure 1 shows the interference of a He-Ne laser probe beam inside a rod. Because of the flashlamp pumping, the temperature of a rod increases and the optical path length

changes. Thereafter, the pumping is suddenly stopped and the optical path length begins to return to the original state via the cooling process. A Nd:YAG rod has two parallel optically polished endfaces, which have a reflectance of 6.6% for 0.633 μm . The transmitted beam (beam 1) and the beam reflected (beam 2) from both endfaces are interfering, and their intensity is modulated with time as the rod is cooled. The relationship between the temperature increase ΔT and the number of fringe shifts S with time at any point is given by

$$\Delta T(r) = \frac{\lambda}{2} \left(L_c \frac{dn}{dT} + nL_0\alpha \right)^{-1} S(r), \quad (1)$$

where λ is the wavelength of the probe beam, L_0 is the length of the rod (152 mm), α is the linear expansion coefficient of the rod ($7.5 \times 10^{-6}/^\circ\text{C}$), n is the refractive index (1.83) at the probe wavelength, and dn/dT is its thermal coefficient ($7.3 \times 10^{-6}/^\circ\text{C}$).¹⁰

The pump pulse is very short compared to the period of heat removal; hence, we can ignore the heat diffusion during the pumping period. The pumping uniformity can be clearly seen from the initial temperature distribution over the cross section of a rod just after single pulse pumping.

Also, the HGR ϕ at a given point inside the rod can be expressed as

$$\phi(r) = mC_p\Delta T(r)V/W, \quad (2)$$

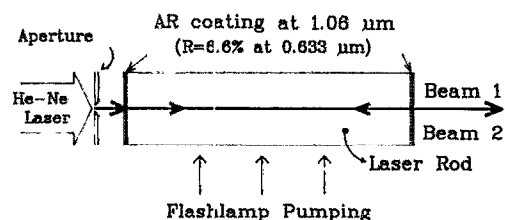


FIG. 1. Interference between beam 1 and beam 2 due to the partial reflectance of two endfaces of the rod.

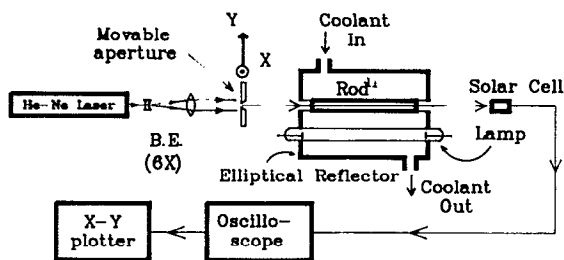


FIG. 2. Experimental setup for the measurement of the temperature inside of a Nd:YAG rod.

where m is the mass density of the rod (4.56 g/cm^3), C_p is the specific heat of the rod ($0.59 \text{ W s/g}^\circ\text{C}$), V is the rod volume, and W is the flashlamp input power.¹⁰

At a high input power and high repetition rate pulsed operation, the rod is cooled down and the radial heat flow changes the initial temperature distribution to a parabolic temperature profile. Consequently, this makes the rod behave like a thick positive lens. This lens effect focuses the probe beam to the optical axis of the rod.² Therefore, the measurement of the temperature is almost impossible except at the rod center because the overlap of two interfering beams is difficult to predict at other parts of the rod. The steady-state temperature distribution at any point along the radial direction can be expressed by the following equation:¹⁰

$$T(r) - T_c = \frac{\phi(r)W}{2\pi a L_0} \left(\frac{a^2 - r^2}{2Ka} + \frac{1}{h} \right), \quad (3)$$

where T_c is the coolant temperature, a is the radius of rod (3.6 mm), and h is the SHTC. If the HGR $\phi(0)$ are measured using Eq. (2), the temperature distribution of the rod can be obtained from Eq. (3). Also from Eq. (3), the knowledge of $T(0)$ and $\phi(0)$ provide the SHTC, which determines the temperature difference between the rod surface and the coolant.

Figure 2 shows the experimental setup used for measuring the temperature inside a rod for a single pulse and a high repetition rate pulsed operation. A single elliptical gold-plated pumping reflector, whose elliptical axes are 19.0 and 16.5 mm in length, was fabricated in this laboratory. An expanded ($6\times$) 5 mW He-Ne laser beam was incident on the rod through an X-Y movable aperture with a 1 mm diameter located in front of the rod. A solar cell detector was used for counting the interference fringe shift.

The initial temperature distributions along the x axis, which connects the lamp and rod center, and y axis were measured just after the single pulse pumping to evaluate the degree of the pumping uniformity. Figure 3(a) shows that an asymmetric temperature distribution exists along the x axis. This effect is due to direct pumping from the lamp in the closed-coupled configuration of the pumping reflector. There is a symmetric temperature distribution with respect to the y axis [Fig. 3(b)]. As the pumping light impinges on the rod center, the pumping light is absorbed by the medium. For the present reflector, we could see that the heat deposited at the outer edge was about 20% larger

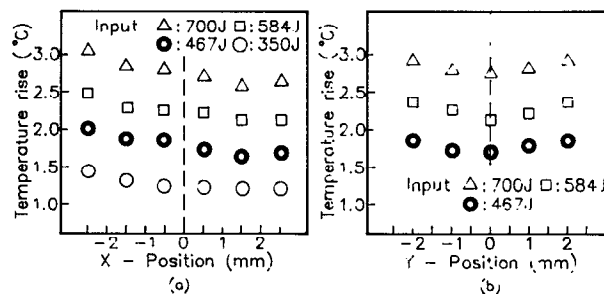


FIG. 3. Initial temperature distributions of a Nd:YAG rod along the (a) x axis, (b) y axis just after single pulse pumping.

than that of the center. This means that the rod acts as a negative lens at the initial pumping stage.

The heat generation rate depends on the pumping geometry, the reflectance of the reflector wall, and spectral distribution of the pumping light, etc. In this experiment, the average value of the HGR ϕ was $5\% \pm 0.5\%$. This value is lower than those from previous works.^{5,11} Perhaps this is due to the poor reflectivity of our pumping reflector wall.

The temperature of the rod center was measured by counting the number of interference fringe shifts using Eq. (1). Figure 4(a) shows the temperature at the rod center as a function of the cooling water flow rate. As the water flow rate increases, the temperature at the rod center decreases. In the case of high power pumping, it is difficult to measure the temperature at the rod center with this technique because there are too many fringe shifts (order of $\sim 10^2$) to count within a short temperature relaxation time, typically 1 s. In this case, the SHTC has to be determined in order to calculate the temperature at the rod center. It is clear from Eq. (3) that if we know $T(0)$ from Fig. 4(a) and the HGR $\phi(0)$, the SHTC can be easily calculated. Also, the SHTC can be calculated from Hsu's equation⁶ which is valid for laminar and turbulent flow, and is presented in the Appendix. Figure 4(b) shows the measured and theoretical values of the SHTC as a function of the cooling water flow rate. The coolant flowmeter of

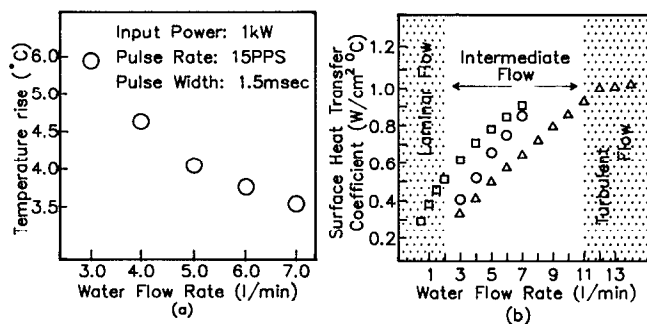


FIG. 4. (a) Temperature rise of the rod center as a function of the water flow rate after a high repetition rate pulsed operation. (b) Measured values of the SHTC as a function of water flow rate with calculated values from Hsu's equation: (\square) calculated values from Eq. (A1), which are valid for the laminar flow region shaded with dots; (\circ) measured values from this simple interferometric technique; (\triangle) calculated values from Eq. (A2), which are valid for the turbulent flow region shaded with dots.

coolant in our experiment indicated that we were in an intermediate flow region. The experimental values are well matched with the interpolated values obtained through Eqs. (A1) and (A2) in the intermediate flow. With the HGR parameter, the calculated SHTC allows the scaling of the rod temperature up to multikilowatt pumping powers.

In conclusion, the initial temperature distribution of a rod was measured along the two orthogonal axes just after single pulse operation. This result is also applicable in evaluating the influence of a pumping reflector geometry on the pumping uniformity inside a rod. The temperature increase of the rod center was measured interferometrically in high repetition rate pulsed operation with a moderate input power. With the HGR, this result determines the temperature profile of a rod in moderate input power and is used to deduce the SHTC, which is an important parameter used to predict the temperature distribution of the rod at a higher power input.

Appendix. The surface heat transfer coefficient h can be calculated using the following equations:

Laminar flow: $900 < N_{Re} < 2000$,

$$h = 1.02 \frac{K_W}{D_2 - D_1} N_{Re}^{0.45} N_{Pr}^{0.5} N_{Gr}^{0.05} \left(\frac{D_2 - D_1}{L_0} \right)^{0.4} \left(\frac{D_2}{D_1} \right)^{0.8} \quad (\text{A1})$$

Turbulent flow: $12\,000 < N_{Re} < 220\,000$,

$$h = 0.02 \frac{K_W}{D_2 - D_1} N_{Re}^{0.8} N_{Pr}^{0.33} \left(\frac{D_2}{D_1} \right)^{0.53} \quad (\text{A2})$$

TABLE I. Parameters for SHTC calculation.

Property	Values and units	
K_w ^a : thermal conductivity of the coolant	6×10^{-3}	$\text{W cm}^{-1} \text{ } ^\circ\text{C}^{-1}$
D_1 : rod diameter	6.35	mm
D_2 : inner diameter of the cooling jacket	13.0	mm
ρ : mass density of the coolant	1.0	g/cm^3
u : fluid velocity $4V/[\pi(D_2^2 - D_1^2)]$
V : volumetric flow
μ : viscosity	10^{-2}	$\text{g cm}^{-1} \text{ s}^{-1}$
C_w : specific heat of the coolant	1.0	$\text{W s g}^{-1} \text{ } ^\circ\text{C}^{-1}$
g : gravitational constant	981.0	cm/s^2
γ : volumetric thermal expansion coefficient	6.4×10^{-5}	$^\circ\text{C}^{-1}$

^aReference 6.

where the Reynolds number is $N_{Re} = [\rho u(D_2 - D_1)]/\mu$, the Prandtl number is $N_{Pr} = C_w \mu / K_w$, and the Grashof number is $N_{Gr} = \{(D_2 - D_1)^3 \rho^2 g \gamma [T(a) - T_c]\} / \mu^2$. The parameters for SHTC calculation are listed in Table I.

¹S. Sims, A. Stein, and C. Roth, *Appl. Opt.* **5**, 621 (1966).

²E. Riedel and G. Baldwin, *J. Appl. Phys.* **38**, 2720 (1967).

³A. Y. Cabezas, L. G. Komai, and R. P. Treat, *Appl. Opt.* **5**, 647 (1966).

⁴M. S. Mangir and D. A. Rockwell, *IEEE J. Quantum Electron.* **22**, 574 (1986).

⁵K. Mann and H. Weber, *J. Appl. Phys.* **64**, 1015 (1988).

⁶W. Koechner, *J. Appl. Phys.* **44**, 3162 (1973).

⁷U. O. Farrukh, A. M. Buoneristiani, and C. E. Byvik, *IEEE J. Quantum Electron.* **24**, 2253 (1988).

⁸F. Docchio, L. Pallaro, and O. Svelto, *Appl. Opt.* **24**, 3752 (1985).

⁹I. Y. Milev, S. S. Dimov, S. Z. Kurtev, O. E. Denchev, and I. P. Angelov, *Appl. Opt.* **29**, 772 (1990).

¹⁰W. Koechner, *Solid State Laser Engineering* (Springer, New York, 1976), Chaps. 2 and 7.

¹¹W. Koechner, *Appl. Opt.* **9**, 1429 (1970).